

Study on the stability of mine roadways supported by rock bolts and shotcrete in jointed rock masses

Ngoc Thai Do^{1*}, Trong Hung Vo², Anatoliy Grigoryevich Protosenya³, Van Quang Nguyen⁴

¹ Faculty of Civil Engineering, Hanoi University of Mining and Geology, Hanoi, Vietnam

² Faculty of Civil Engineering, Hanoi University of Mining and Geology, Hanoi, Vietnam

³ Faculty of Civil Engineering, Saint-Petersburg Mining University, Russia

⁴ Faculty of Civil Engineering, University of Transport Technology, Hanoi, Vietnam

* Corresponding email: dongochai@humg.edu.vn

Abstract: *In recent years, to ensure sufficient coal output for economic development, a significant number of coal mine roadways have been constructed annually in Vietnam's underground coal mines. The coal mine roadways are constructed through different rock conditions, such as soft rock and rock hard with jointed rock masses. The jointed rock masses affect the stability of the mine roadways. Therefore, designing and constructing support systems to maintain the stability of these roadways is important. This study employs the finite element method to assess the stability of a mine roadway supported by rock bolts and shotcrete, constructed within jointed rock masses. The results of the study presented the displacement values, strength factor and failure of the rock mass around mine roadway, as well as the axial force in rock bolts and shotcrete, and the paper also investigated the influence of the inclination angle of the jointed rock masses and the discontinuity spacings for jointed rock masses on the stability of the mine roadway.*

Keywords: *coal mine, mine roadway, rock bolts, shotcrete, jointed rock masses*

1. Introduction

Rock mass instability in underground mining roadways poses a significant risk to the safety of personnel and equipment. The stability of a roadway is influenced by various factors, including the geological composition of the surrounding rock mass, the magnitude of in-situ stresses, and the geometric parameters of the roadway such as its shape, size, and construction methodology. The mechanical stability of the rock mass surrounding the roadway is primarily governed by the stress distribution and structural conditions within the rock. In roadways excavated in fractured rock at shallow depths, the most common failure mechanisms involve the detachment of rock wedges from the roof or sidewalls of the roadway. These wedges form due to the intersection of structural discontinuities, such as joints and bedding planes, which divide the rock mass into discrete, interconnected blocks [1-2]. During excavation, the removal of material creates a free surface, reducing the confining support from the surrounding rock. If the intersecting planes are continuous or if rock bridges along these discontinuities are weakened or broken, the detached wedges may either fall or slide, leading to localized instability. If appropriate stabilization measures are not applied to secure loose rock wedges, the stability of the rock mass surrounding the roadway may rapidly degrade. The displacement of any wedge, whether through falling or sliding, diminishes the cohesion and confinement of the rock mass [3-4]. This reduction in mechanical support can lead to a cascading failure, as neighboring wedges become increasingly prone to dislodgement, further compromising the structural stability of the roadway. The mechanical behavior of a rock mass during underground excavation is influenced by the relationship between the excavation scale and the characteristic block size or joint spacing. Depending on this scale, the rock mass strength can be treated as either isotropic, where strength properties are uniform regardless of location or orientation, or anisotropic, where strength varies with loading direction. In mining roadways, particularly those excavated through fractured rock masses, stabilization techniques such as anchors and shotcrete are highly effective [5-7]. Advancements in rock bolting technologies have been paralleled by significant theoretical and practical achievements. Extensive theoretical analyses, laboratory experiments, numerical simulations, and in-situ testing have provided a deeper understanding of the intrinsic mechanisms of rock bolting. This progress has fueled the continuous development of more efficient and reliable rock bolting techniques [8-12]. Extensive engineering practice has demonstrated that bolt-grouting combined support technology significantly enhances the strength of the surrounding rock and the load-bearing capacity of the support structures. This method effectively controls large deformation failures and rheological behavior in deep, soft rock roadways subjected to high stress. As a result, bolt-grouting combined support contributes to maintaining the long-term stability and safety of these roadways [13, 14]. The integration of computer-based finite element analysis (FEM) has

revolutionized the design process for underground excavations. FEM software, such as Phase², enables engineers to compute and compare roadway deformations and stress distributions, assess the interaction between support systems and the excavated rock mass, and verify the accuracy of empirically derived excavation and support system designs [15-17]. This paper utilizes the finite element method with the Phase² model to investigate the stability of the rock mass surrounding the roadway. The roadway is constructed within a fractured rock mass and supported by a structure comprising rock bolts and shotcrete.

2. Geological background

This study aims to evaluate the stability of the roadway, focusing on the influence of joints in sandstone. The tunnel measures 3480 mm in height and 4800 mm in width, with the geotechnical properties of the sandstone and joints provided in Tables 1 and 2.

Tab. 1. Geotechnical properties of sandstone

No	Parameters	Symbol	Values	Units
1	Unit weight	ρ	0.0265	(MN/m ³)
2	Young's modulus	E	6.15	(GPa)
3	Poisson's ratio	ν	0.28	-
4	Tensile strength	σ_t	0.65	(MPa)
5	Friction angle	φ	36	(°)
6	Cohesion	c	0.35	(MPa)

Tab. 2. Geotechnical properties of joints in rock mass

No	Parameters	Symbol	Values	Units
1	Inclination angle	β	35	(°)
2	Spacing	l	1.0	(m)
3	Tensile strength	σ_{tj}	0.00005	(MPa)
4	Cohesion	c_j	0.2	(MPa)
5	Friction angle	φ_j	25	(°)
6	Normal stiffness	K_n	150000	(Mpa/m)
7	Shear stiffness	K_s	15000	(Mpa/m)

The roadway is supported by rockbolts and shotcrete, as illustrated in Figure 1. Each rockbolt has a diameter of 22 mm, a length of 2500 mm, and an out-of-plane spacing of 1 m. The shotcrete layer is 70 mm thick.

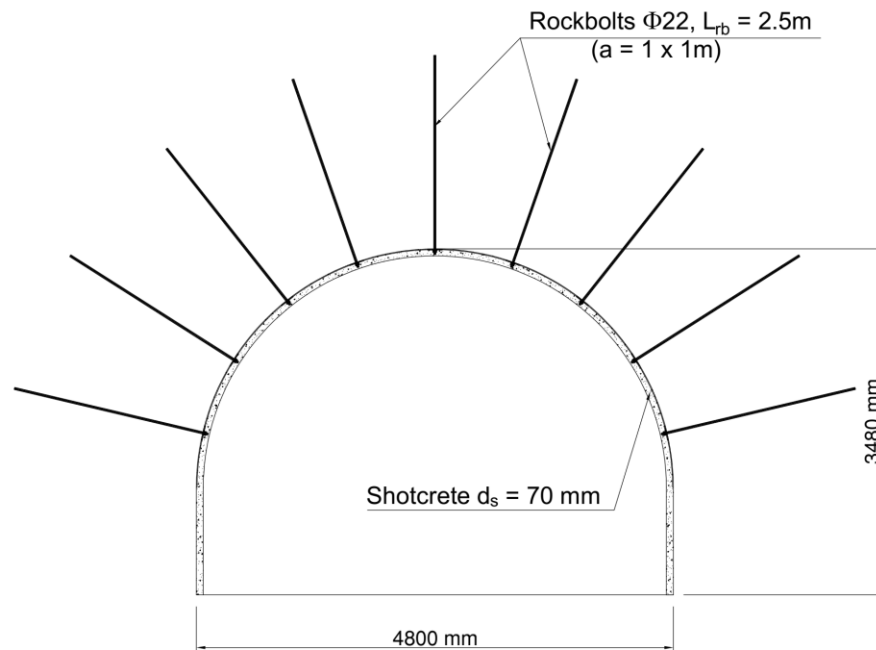


Fig. 1. The cross-section of the tunnel, including rockbolts and shotcrete was incorporated into the simulation model

A pattern of mechanically anchored rockbolts, 2.5 m in length and 22 mm in diameter, was installed on a 1 m x 1 m grid in the arch of the roof and upper sidewalls. The mechanical properties of the rockbolts are presented in Table 3.

Tab. 3. Mechanical parameters of rockbolts

N ₀	Parameters	Symbol	Values	Units
1	Rock bolt diameter	Φ	22	(mm)
2	Rock bolt length	L _{rb}	2500	(mm)
3	Rock bolt Modulus	E _{rb}	280	(GPa)
4	Tensile capacity	F _t	0.5	(MN)
5	Residual Tensile capacity	F _{t,Rd}	0.01	(MN)
6	Out-of-plane Spacing	l'	1000	(mm)

The roadway is supported by an additional shotcrete layer that is 70 mm thick. The technical characteristics of this shotcrete layer are presented in Table 4.

Tab. 4. Technical characteristics of shotcrete

N ₀	Parameters	Symbol	Values	Units
1	Density	ρ _s	2500	(kg/m ³)
2	Young's modulus	E _s	27	(GPa)
4	Poisson's ratio	ν _s	0.2	-
5	Thickness	d _s	70	(mm)
6	Compressive yield strength	f _c	35	(MPa)
7	Tensile yield strength	f _t	3.0	(MPa)
8	Residual yield strength	f _{t,rd}	0	(MPa)

3. Methodology

The application of Rocscience's Phase² model allows for a reliable assessment of the location and extent of the rock failure zone around the roadway [19]. This Phase² model also allows for the assessment of the effectiveness of the application of supporting components, such as rockbolts and shotcrete to improve the stability of the rock mass around the roadway.

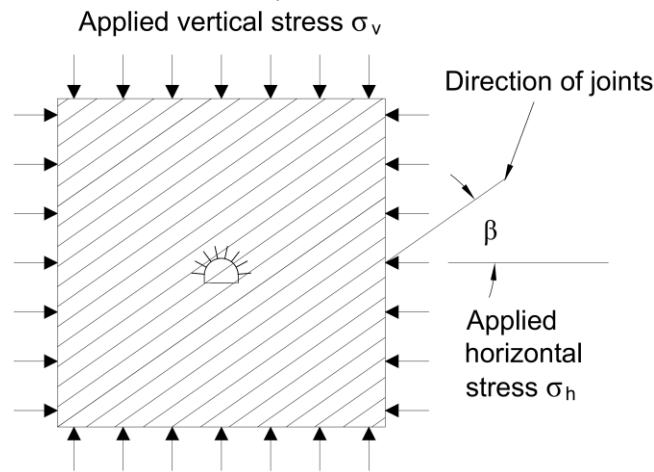


Fig. 2. Diagram of the stress forces acting on the roadway [20]

The roadway is located at a depth of 120 m below ground level. The principal vertical stress, σ_v , is calculated using the formula [20]: $\sigma_v = \gamma \cdot z$, where σ_v is the vertical stress, γ is the unit weight of the overlying rock, and z is the depth below the surface. The horizontal stress in the model is determined by the formula [21]: $\sigma_h = k \cdot \sigma_v$, where k is a factor, $k = 0.25 + 7 \cdot E_h \left(0.001 + \frac{1}{z}\right)$, and E_h is the average deformation modulus of the upper crust measured in the horizontal direction. A schematic diagram of the calculation model is presented in Figure 2.

The analytical model has dimensions of 80 m x 80 m. The Mohr-Coulomb failure criterion is employed to simulate the plastic behavior of the rock masses. Initial stresses are applied to the model, as shown in Figure 2. Default boundary conditions are employed, with the external boundaries constrained by a fixed condition (i.e., zero displacement). The steps to implement the model are as follows:

- Step 1: Set up initial conditions;
- Step 2: Apply initial stress;
- Step 3: Construct the roadway and install rock bolts with shotcrete;
- Step 4: Export the analysis results.

4. Results and discussion

Figures 3 to 7 present the principal stresses (σ_3), displacements, and durability of the rock mass around the roadway, as analyzed using the Phase² model. The results indicate that, following support from rockbolts and shotcrete, the principal stress (σ_3) in the rock mass surrounding the roadway increases, while the displacement decreases, thereby enhancing the durability factor. The principal stresses (σ_3) around the roadway are illustrated in Figures 3 and 4.

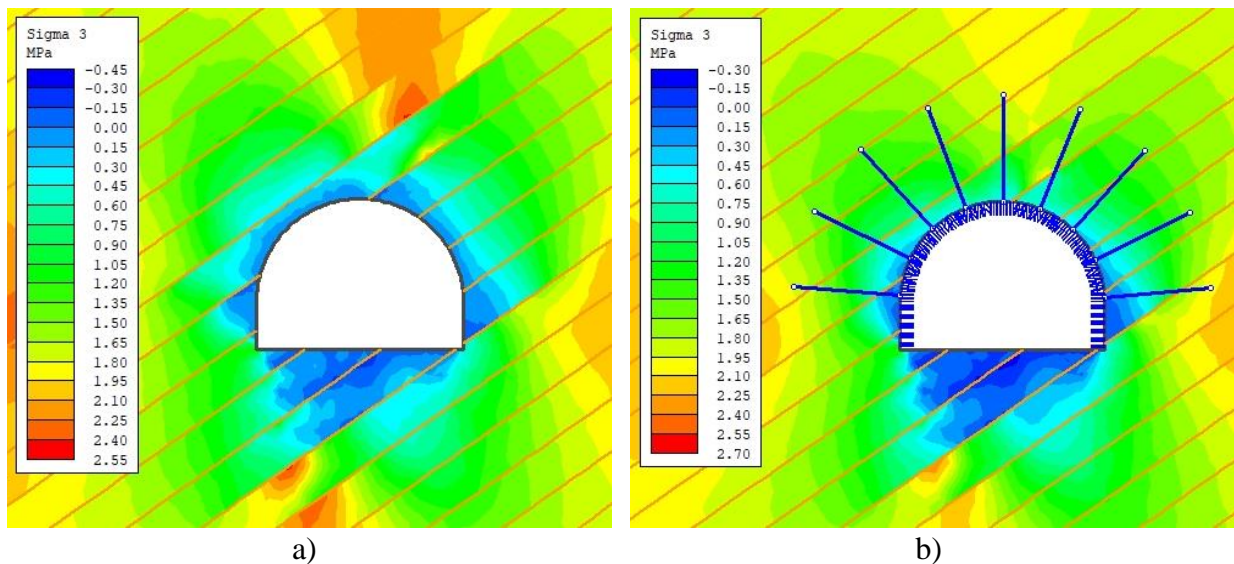


Fig. 3. Contours of mean principal stress (σ_3) in the rock mass around the unsupported roadway (a) and supported roadway (b)

The types of instability problems that can arise in unsupported excavations are illustrated in Figure 3a. In this scenario, the rock mass is relatively closely jointed, and as a result of blasting in adjacent stopes, small wedges and blocks have fallen from the roadway roof. Figure 3a also displays the principal stress (σ_3) in the rock mass around both the unsupported and supported roadways. In contrast, Figure 3b shows the roadway where support has been installed, featuring rock bolts placed in a pattern along the roof and upper sidewalls. The entire roadway surface is then covered with a layer of shotcrete approximately 70 mm thick.

In the roadway with installed rockbolts and shotcrete, the principal stress (σ_3) around the roadway boundary is significantly higher. Specifically, the maximum principal stress at the roadway roof increases (σ_3) from 0.243 MPa to 1.21 MPa upon the installation of the support structure.

Figure 4 presents the distribution of principal stress (σ_3) around the roadway boundary. The results indicate that the principal stress (σ_3) in the supported roadway is greater than that in the unsupported roadway. Notably, at the roadway roof, the principal stress in the supported roadway shows the most significant increase compared to the unsupported roadway.

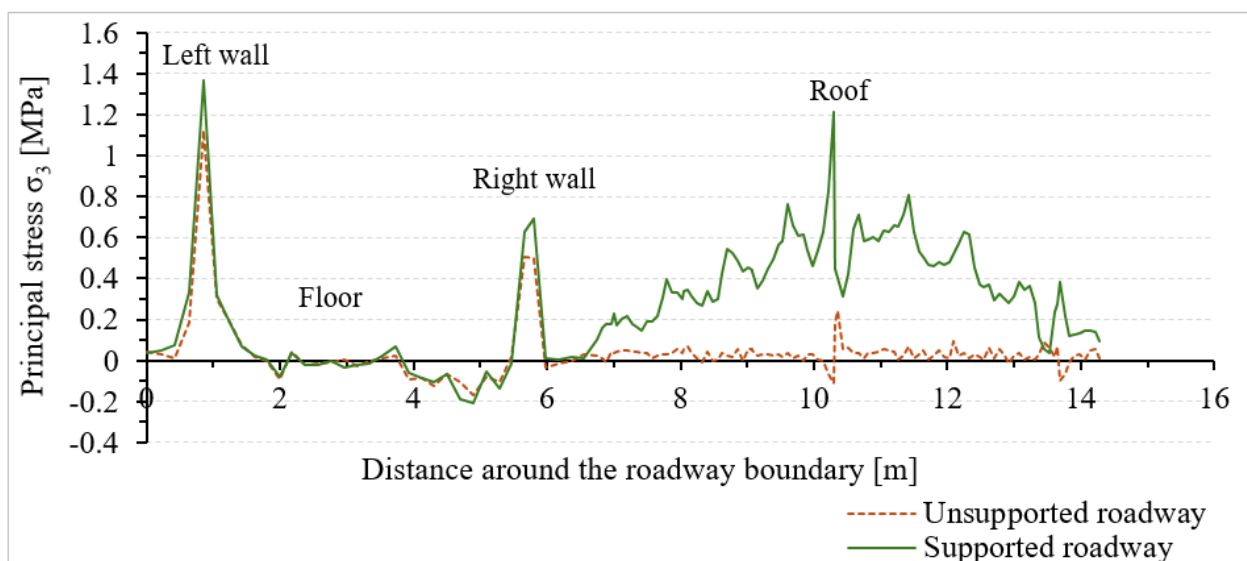


Fig. 4. Distribution of principal stress (σ_3) around the roadway boundary

The total displacements in the rock surrounding both the unsupported and supported roadways are presented in Figures 5 and 6.

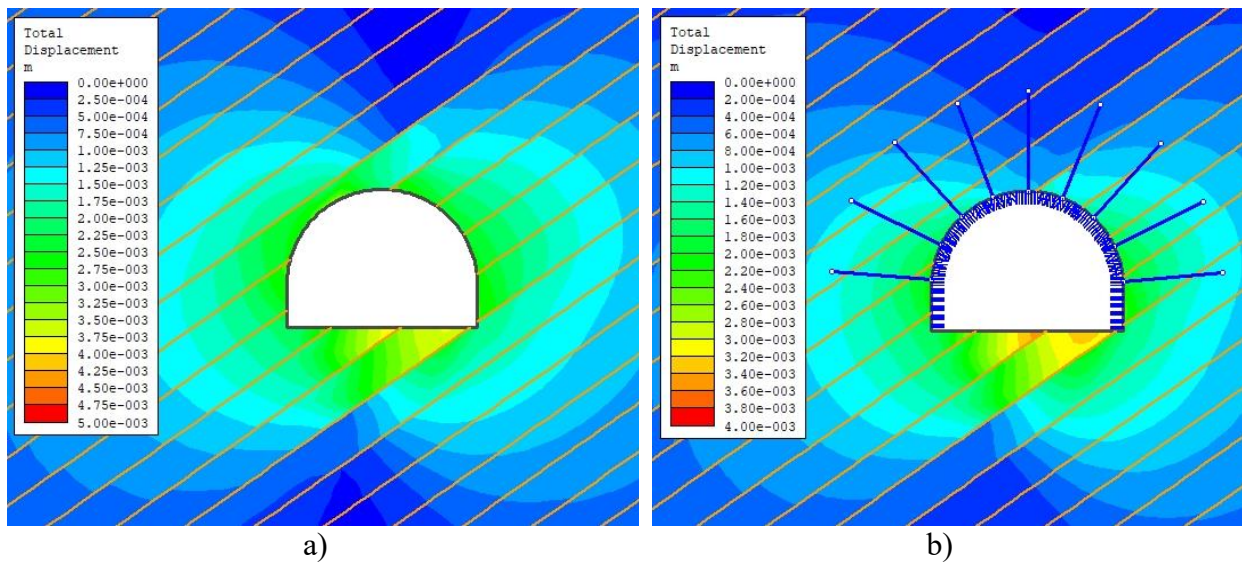


Fig. 5. Total displacements in the rock mass around the unsupported roadway (a) and the supported roadway (b)

Figure 5a illustrates the displacement in the rock mass around the unsupported roadway, where the maximum displacement at the roof is approximately 3.3 mm, while the displacement at the floor is about 4.1 mm. In contrast, Figure 5b shows the total displacement in the rock mass around the supported roadway, indicating a reduction in displacement values due to support. Specifically, the roof displacement decreased from 3.3 mm to 1.20 mm, and the floor displacement decreased from 4.1 mm to 3.6 mm. The study results reveal that the maximum floor heave is 3.6 mm.

Figure 6 illustrates the total displacements in the rock around both the unsupported and supported roadways. The results indicate that the displacement of the rock surrounding the supported roadway is less than that of the unsupported roadway. Notably, at the roadway roof, the displacement around the supported roadway is significantly reduced compared to the unsupported roadway. This reduction is attributed to improved stress distribution resulting from the slight arching of the roof.

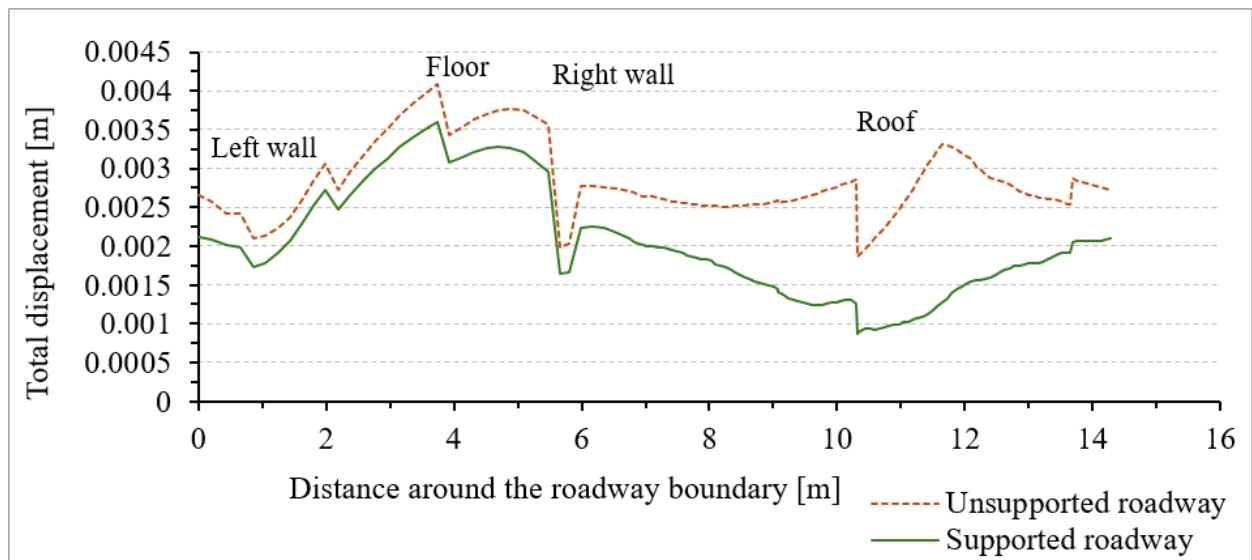


Fig. 6. Distribution of total displacement around the roadway boundary

The tension strength factor of Phase², as shown in Figure 7, illustrates that the structural orientation of joint elements can either clamp them, leading to failure through the rock mass, or allow them to shear, thus influencing the stress field around the roadway boundary. This interaction affects the rock mass's strength, resulting in a failure mechanism characterized by a combination of shear and tensile yield. The simulation also indicated a significant reduction in the safety factor, approaching or falling below one, along and near the periphery of the circular roadway. Figure 7 further demonstrates that the area with a safety factor below 1 at the roadway roof decreases when the roadway is supported.

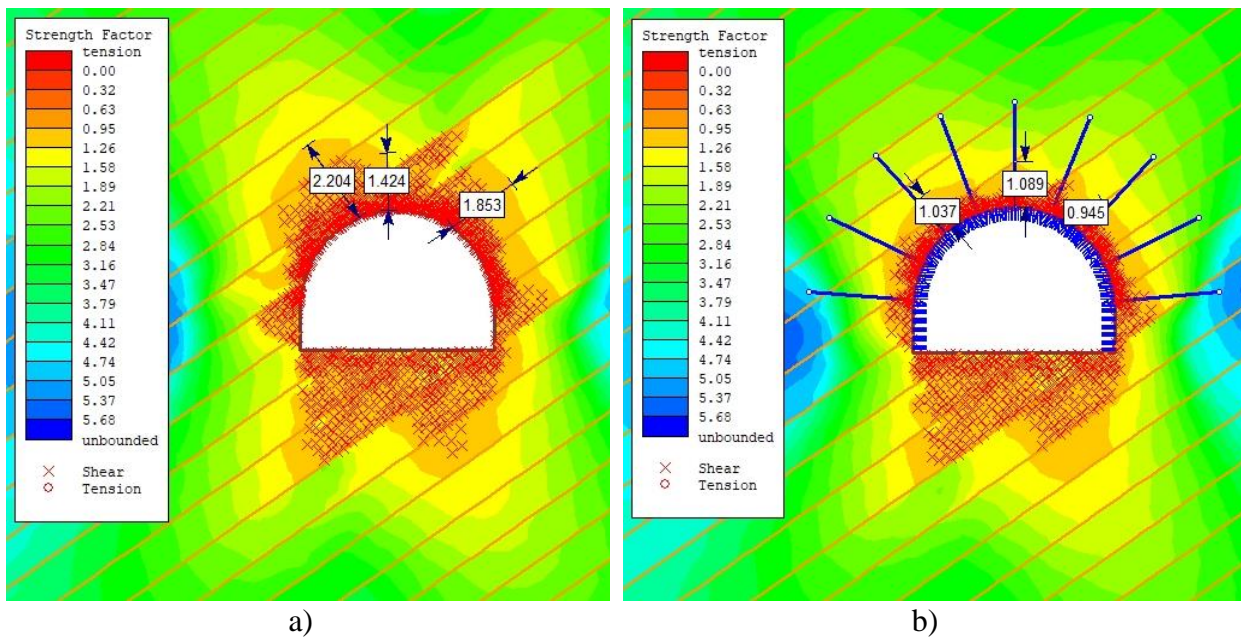


Fig. 7. Strength factor around the unsupported roadway (a) and the supported roadway (b)

In mine roadways excavated in jointed rock masses, the most common failure types involve wedges falling from the roof or sliding out from the side walls of the openings. These wedges are formed by intersecting structural features, such as the roof, side walls, floor, and joints, which divide the rock mass into susceptible wedges, leading to unsafe mining conditions.

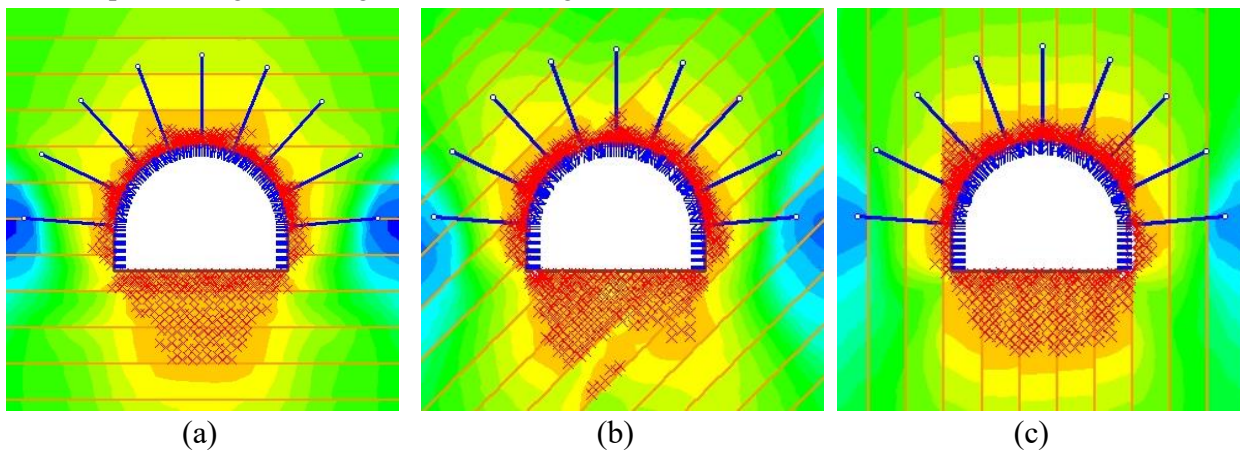


Fig. 8. Strength factor around the roadway for joint inclination angles: $\beta = 0^\circ$ (a), $\beta = 45^\circ$ (b), $\beta = 90^\circ$ (c)

The inclination angle of the joints in the rock mass also significantly impacts the stability of the rock around the roadway boundary. To investigate the influence of joint inclination angles on the principal stress and displacement of the rock surrounding the roadway boundary, the authors conducted research with joint inclination angles of $\beta=0^\circ$, $\beta=45^\circ$, and $\beta=90^\circ$.

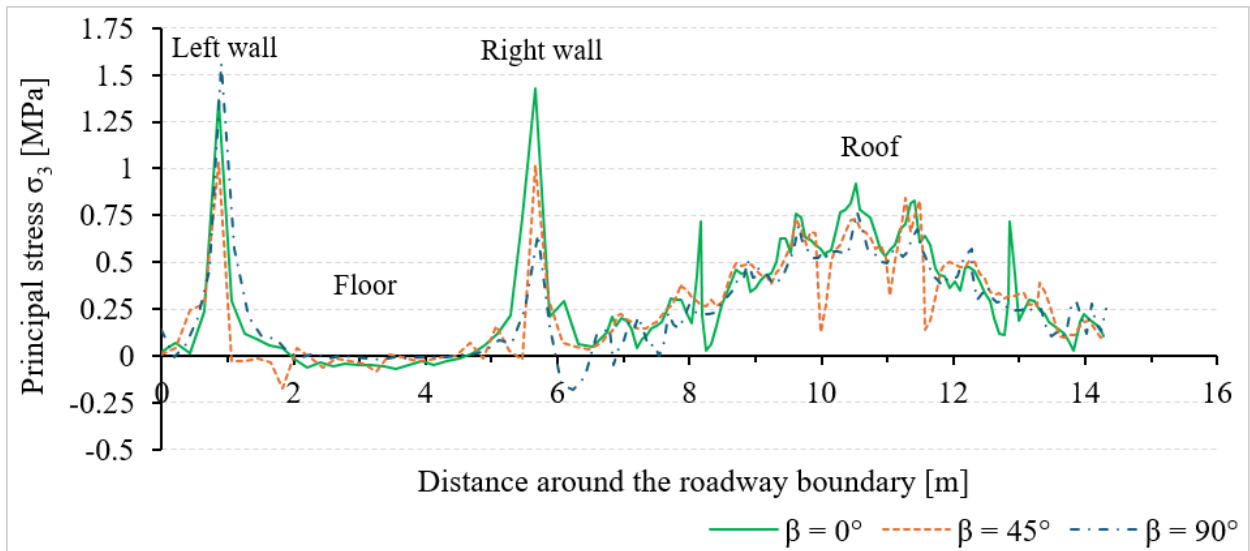


Fig. 9. Distribution of principal stress (σ_3) around the roadway boundary for joint inclination angles of 0° , 45° , and 90°

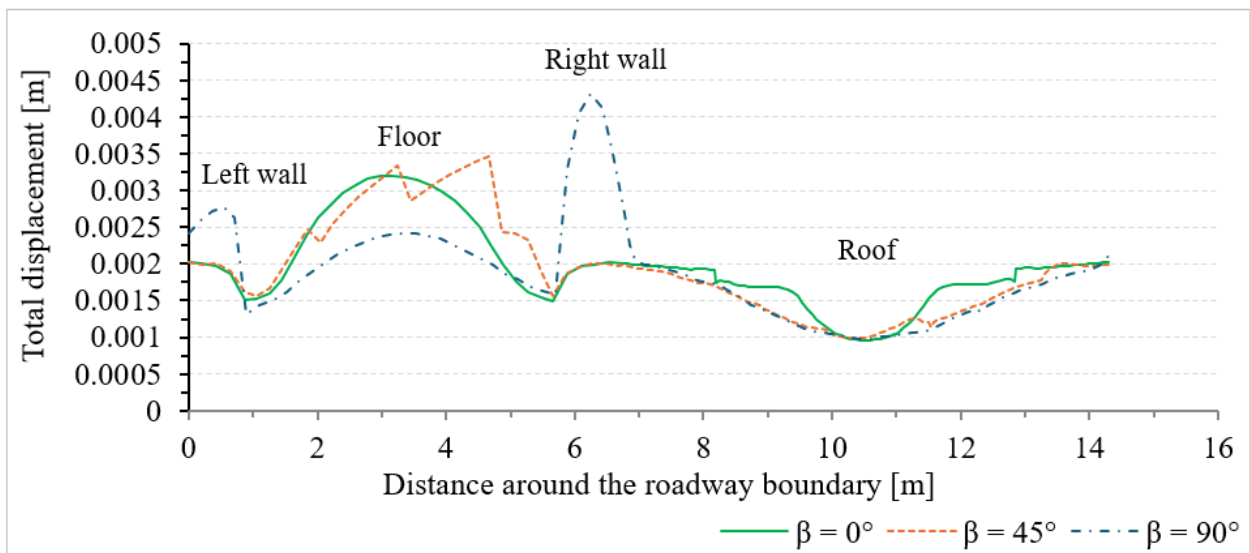


Fig. 10. Distribution of total displacement around the roadway boundary for joint inclination angles of 0° , 45° , and 90°

The principal stress σ_3 around the roadway boundary for joint inclination angles of 0° , 45° , and 90° are presented in Figures 9. The results indicate that the maximum principal stress (σ_3) is 1.56 MPa when the joint angle with respect to the horizontal plane is 90° , occurring between the left wall and the roadway roof. At the roadway roof, the maximum stress is 0.92 MPa when the joint angle is 0° .

The results indicate that the maximum rock displacement around the roadway boundary is 0.43 mm when the joint angle with the horizontal plane is 90° , occurring between the right wall and the roadway roof. At the roadway floor, the largest displacement is 0.35 mm when the joint angle is 45° . To investigate the effect of joint spacing, the research team conducted calculations using a fixed joint inclination angle of 35° and varying joint spacings of 0.5 m, 1.0m, 1.5m. The results, showing the rock strength factor around the roadway for these different spacings, are presented in Figure 11.

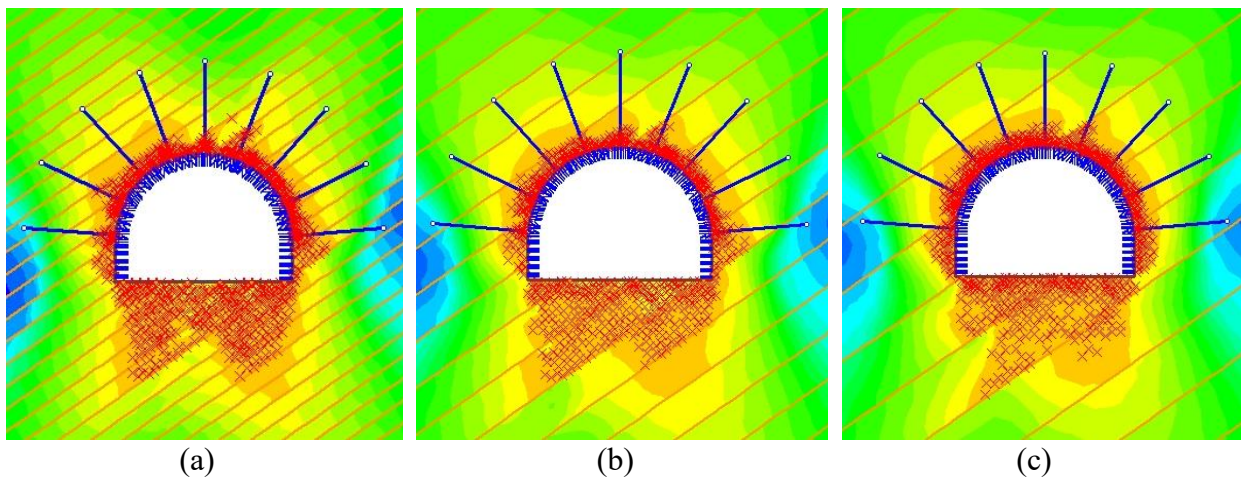


Fig. 11. Strength factor around the roadway for joint spacings: $l = 0.5\text{m}$ (a), $l = 1.0\text{m}$ (b), $l = 1.5\text{m}$ (c)

Figure 12 shows the distribution of principal stress (σ_3) around the roadway boundary. The results indicate that the maximum principal stress (σ_3) in the studied cases is 1.38 MPa, occurring between the right wall and the roadway roof when the joint spacing is $l=1.5\text{ m}$. At the roadway roof, the largest (σ_3) is 1.33 MPa when the joint spacing is $l=0.5\text{m}$.

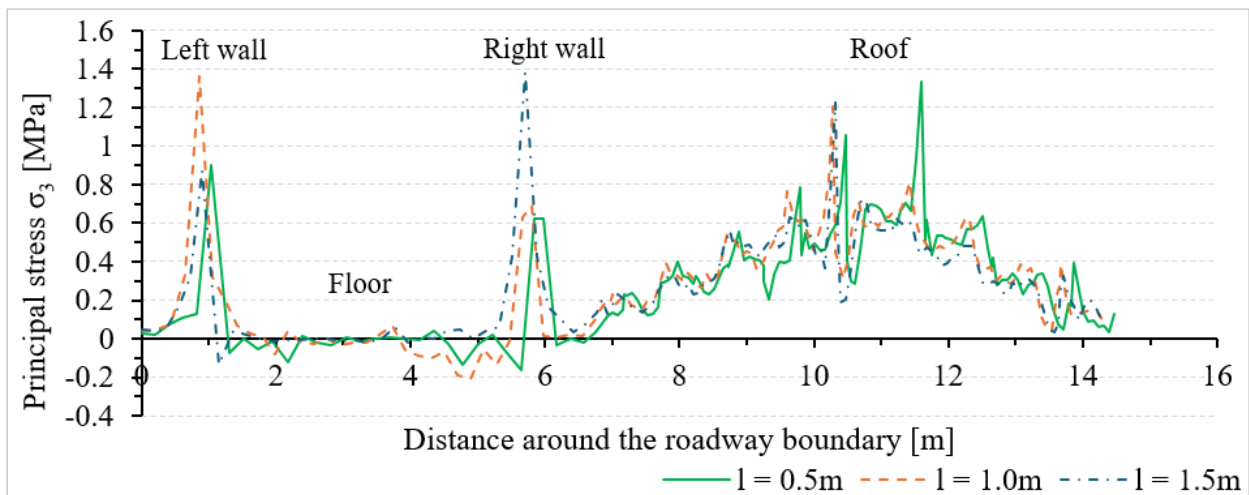


Fig. 12. Distribution of principal stress (σ_3) around the roadway boundary for joint spacings of 0.5 m, 1.0 m, and 1.5 m

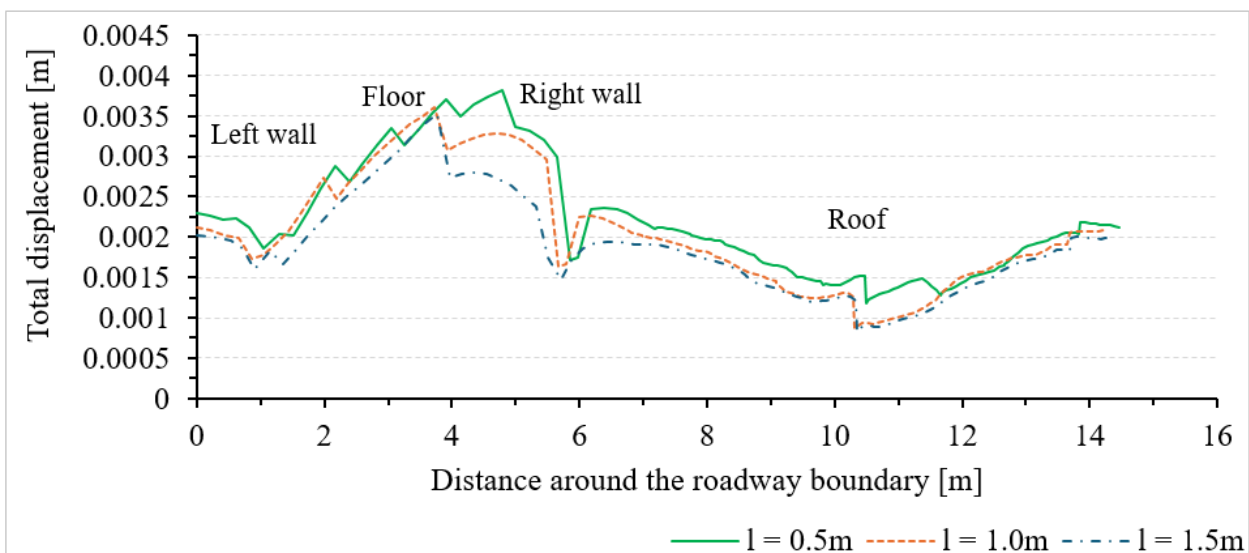


Fig. 13. Distribution of total displacement around the roadway boundary for bedding joint spacings of 0.5 m, 1.0 m, and 1.5 m

The total displacement around the roadway boundary for bedding joint spacings of 0.5 m, 1.0 m, and 1.5 m, are presented in Figure 13. The results indicate that the maximum displacement values for joint spacings of 0.5 m, 1 m, and 1.5 m are 0.38 mm, 0.36 mm, and 0.35 mm, respectively. At the roadway roof, the largest displacement, 2.1 mm, occurs when the joint spacing is 0.5 m.

5. Conclusion

Rockbolts and shotcrete support systems are effective in stabilizing mining roadways constructed in jointed rock masses. The inclination angle and spacing of joints within the rock mass influence the principal stress (σ_3) and the displacement of the rock surrounding the roadway boundary. Based on the analyzed tunnel conditions, the following conclusions have been drawn:

The installation of rockbolts and shotcrete significantly reduces the displacement of the rock mass around the roadway boundary, thereby decreasing the size of the zone with a strength coefficient less than or equal to 1.

The inclination angle of the joints in the rock mass affects both the principal stress (σ_3) and the displacement around the roadway boundary. When the joint inclination is 0° , the principal stress (σ_3) in the roadway roof is maximized. In contrast, at the roadway walls and foundation, the principal stress is greatest when the joint inclination is 90° . The rock displacement around the roadway boundary is also highest when the joint inclination is 90° .

Joint spacing within the rock mass also influences the principal stress (σ_3) and displacement. When the joint spacing is 1.5m, the principal stress is at its maximum. However, the displacement around the roadway boundary is largest when the joint spacing is 0.5m.

Literature - References

1. Bewick R.P., Kaiser P.K., Amann F., 2019. The Strength of Massive to Moderately Jointed Rock and its Application to Cave Mining. *Journal of Rock Mechanics and Geotechnical Engineering* 11, 562-575.
2. Kovalevska I., Barabash M., & Snihur, V., 2018. Development of a research methodology and analysis of the stress state of a parting under the joint and downward mining of coal seams. *Mining of Mineral Deposits*, 12(1), 76-84. <https://doi.org/10.15407/mining12.01.076>
3. Bewick RP, Kaiser PK, Amann F., 2019a. Strength of massive to moderately jointed hard rock masses. *J Rock Mech Geotech Eng*. <https://doi.org/10.1016/j.jrmge.2018.10.003>
4. Bewick R.P., 2021. The Strength of Massive to Moderately Jointed Rock and its Application to Cave Mining. *Rock Mech Rock Eng* 54, 3629–3661. <https://doi.org/10.1007/s00603-021-024663>
5. Das R., Nath Singh T., 2020. Effect of rock bolt support mechanism on tunnel deformation in jointed rockmass: A numerical approach, *Underground Space* (2020), doi: <https://doi.org/10.1016/j.undsp.2020.06.001>
6. Wang W, Song Q, Xu C, Gong H., 2018b. Mechanical behaviour of fully grouted GFRP rock bolts under the joint action of pre-tension load and blast dynamic load. *Tunnelling and Underground Space Technology*, 73, 82–91.
7. Malmgren L., Nordlund E., 2008. Interaction of shotcrete with rock and rock bolts – Anumerical study. *International Journal of Rock Mechanics & Mining Sciences* 45, 538–553. doi:10.1016/j.ijrmms.2007.07.024
8. Tran T.M., Do N.T., Dang T.T., Nguyen D.P., Vo T.H., 2021. Stabilization of Deep Roadways in Weak Rocks Using the System of Two-level Rock Bolts. *Journal of the Polish Mineral Engineering Society*, No.2, Vol.1, 2021. <http://doi.org/10.29227/IM-2021-02-13>.
9. Guo L., Tao Z., He M., Coli M., 2024. Excavation compensation and bolt support for a deep mine drift. *Journal of Rock Mechanics and Geotechnical Engineering*. 16 (8), pp. 3206-3220.
10. Masny W., Nita Ł., Ficek J., 2022. Case Study of Rock Bolting in a Deep Coal Mine in Poland. *Arch. Min. Sci.* 67 (2022), 1, 79-94. <https://doi.org/10.24425/ams.2022.140703>
11. Wang H., Xiao G., Jiang M., Crosta G.B., 2018a. Investigation of rock bolting for deeply buried tunnels via a new efficient hybrid DEM-Analytical model. *Tunnelling and Underground Space Technology*, 82, 366–379.

12. Li C.C., 2017. Principles of rockbolting design. *Journal of Rock Mechanics and Geotechnical Engineering*, 9(3), 396–414.
13. Chen Y., Meng G., Xu G., Wu H., Zhang G., 2016. Bolt-grouting combined support technology in deep soft rock roadway. *Int. J. Min. Sci. Technol.*, 26 (5), pp. 777-785.
14. Goel R.K., Swarup A., Sheorey P.R., 2007. Bolt length requirement in underground openings. *International Journal of Rock Mechanics and Mining Sciences*, 44(5), 802–811.
15. Riaz, A., Jamil, S. M., Asif M., Akhtar K., 2016. Tunnel support design by comparison of empirical and finite element analysis of the Nahakki tunnel in mohmand agency, Pakistan. *Studia Geotechnica et Mechanica*, Vol. 38, No. 1.
16. Kumar A., Sunil S.M., 2023. Back Analysis of Rock Support and Final-Lining Recommendation for Rock Class C1 of a Tunnel. *International Journal of Engineering Trends and Technology*, vol. 71, no. 1, pp. 79-93. Crossref. <https://doi.org/10.14445/22315381/IJETT V71I1P208>.
17. Majcherczyk T., & Niedbalski Z., 2010. Numerical modeling used for designing of coal mine roadway support. *New Techniques and Technologies in Mining – Proceedings of the School of Underground Mining*, 77-82. <https://doi.org/10.1201/b11329-14>
18. Institute of Mining Science and Technology (IMSAT), 2018. Report: Research on procedures to prevent uplift in the underground workings at the Mao Khe coal mine, Hanoi, Vietnam (2018) (in Vietnamese).
19. RocScience 2010. Phase² finite element modelling software, v.7.0.
20. Hoek E., Kaiser P.K. and Bawden W.F., (1995). *Support of Underground Excavations in Hard Rock*. A. A. Balkema: Rotterdam.
21. Sheorey P.R., 1997. *Empirical rock failure criteria*. Rotterdam: A.A. Balkema.